J Fluoresc (2010) 20:591–597
DOI 10.1007/s10895-009-0590-8

ORIGINAL PAPER

Glycosylated Quantum Dots for the Selective Labelling of *Kluyveromyces bulgaricus* and *Saccharomyces cerevisiae* Yeast Strains

Joël Coulon · Ilan Thouvenin · Fadi Aldeek · Lavinia Balan · Raphaël Schneider

Received: 28 October 2009 / Accepted: 22 December 2009 / Published online: 8 January 2010

Abstract Highly fluorescent CdTe quantum dots (QDs) stabilized by thioglycolic acid (TGA) were prepared by an aqueous solution approach and used as fluorescent labels in detecting yeast cells. Sugars (mannose, galactose or glucose) were adsorbed on CdTe@TGA QDs and the interaction of these nanoparticles with yeast cells was studied by fluorescence microscopy. Results obtained demonstrate that galactose and mannose functionalized QDs associate respectively with *Kluyveromyces bulgaricus* and *Saccharomyces cerevisiae* yeast strains due to saccharide/lectin specific recognition. Glucose-functionalized CdTe QDs, which are not recognized by cell lectins, preferentially localize in the bud scars of *S. cerevisiae.*

Keywords Quantum dots · Cadmium telluride · Yeast · Labelling · Lectins/saccharides selective recognition

J. Coulon (✉) · I. Thouvenin · F. Aldeek
LCPME, Laboratoire de Chimie Physique et Microbiologie pour l'Environnement, Nancy-University, CNRS,
405 rue de Vandoeuvre,
54600 Villers-lès-Nancy, France
e-mail: joel.coulon@pharma.uhp-nancy.fr

R. Schneider (✉)
DCPR, Département de Chimie Physique de Réactions, Nancy-University, CNRS,
1 rue Grandville, BP 20451, 54001 Nancy, France
e-mail: raphael.schneider@ensic.inpl-nancy.fr

L. Balan
DPG, Département de Photochimie Générale, UMR CNRS 7525, Université de Haute Alsace, ENSCMu,
3 rue Alfred Werner,
68093 Mulhouse, France

Introduction

Semiconductor nanocrystal quantum dots (QDs) can be advantageously used as nanoemitters for biological labelling over conventional organic fluorophores [1–6]. Indeed, QDs exhibit robust photochemical stability, high quantum yields, and excellent resistance to chemical and photochemical degradation, as well as size-tunable photoluminescence that ranges from visible to near-IR with sharp spectral bands [7–9]. Moreover, QDs with different emission colors can be simultaneously excited with a single light source, with minimal spectral overlap, thus providing significant advantages for multiplexed detection of molecular targets [10–12].

In recent years, surface-functionalized QDs containing biomolecules such as DNA, proteins, and small molecules have demonstrated a great number of applications in cellular imaging, drug delivery, and as nanosensors [10, 13–15]. Among these biomolecules and due to their important roles in cell growth and development, immune recognition/response, signal transduction, cell-cell communication, …, carbohydrates have been widely associated to QDs for imaging [16–21], targeting [22, 23], and sensing [24–26].

Lectins are proteins or glycoproteins of non-immune origin that bind to mono/oligosaccharides with a high degree of stereospecifity. Lectins have been evidenced not only in plants and animals but also in microorganisms such as bacteria and yeast. The functions of yeast lectins and their ability to recognize a specific saccharide has been well documented [27–29].

Yeasts as many other cells can aggregate, a phenomenon that is known as self-flocculation. The self-flocculation was explained by a lectinic mechanism. A glycoprotein, the lectin, recognizes another specific glycoprotein, the phosphopeptidomannan bore on the adjacent cell [30]. This lectinic

mechanism is favoured by the action of divalent cation [31] and can be inhibited by supplementation of specific carbohydrates. Indeed, mannose and mannose derivatives can inhibit the flocculation of the yeast *Saccharomyces cerevisiae* bearing a mannose specific lectin on its cell wall [32, 33], whereas galactose and galactose derivatives can inhibit the flocculation of the yeast *Kluyveromyces bulgaricus* bearing a galactose specific lectin on its cell wall [34]. This carbohydrate specificity favoured the emergence of new glycoconjugate products, synthesized to identify lectinic receptors [35].

A panel of QDs associated to sugar capable of specifically labelling yeasts according to strain, metabolism, surrounding conditions would be extremely useful for a wide range of applications like the study of complex microbial populations called biofilms. In the current study, we report a cheap and straightforward method for the selective detection of *K. bulgaricus* and *S. cerevisiae* cells using water-soluble CdTe-core QDs associated with galactose and mannose, respectively.

Experimental

Preparation of thioglycolic acid-capped CdTe quantum dots

The chemicals used in the experiments included $CdCl_2$ $2.5H_2O$ (99%), thioglycolic acid (TGA, 99+%), sodium borohydride (96%), tellurium powder (99.9%), and *iso*-propanol (*i*-PrOH, HPLC grade). All chemicals were used without further purification.

The method for the preparation of CdTe@TGA QDs was adapted from [36, 37] with slight modifications. Briefly, 0.071 mg of $CdCl_2{\cdot}2.5\ H_2O$ (0.31 mmol) was dissolved in 250 mL of Milli-Q water deareated with N_2, and 104 µL (1.5 mmol) of TGA was added. Dropwise addition of 1 N NaOH was then used to adjust the pH to 8.2 under vigorous stirring. The solution was then placed in a 500 mL four-neck flask with rubber septa, a thermometer, a condenser, and a stirbar. Deareation was further performed under a robust flow of N_2 for 30 min. An oxygen-free aqueous solution of NaHTe (0.310 µL), freshly prepared by reaction of $NaBH_4$ (13.2 mmol) with tellurium powder (5 mmol) in 10 mL water, was then added to the mixture. The molar ratio of Cd^{2+}/HTe^{-}/TGA was fixed at 1/0.5/2.4. CdTe nanoparticles began to growth during the refluxing and was monitored by UV-vis absorption. After cooling to room temperature, the crude CdTe@TGA solution was concentrated about two-fold using a rotary evaporator. CdTe@TGA QDs were isolated from non-reacted precursors by precipitation using a bad solvent, *i*-PrOH, to narrow the particle size distribution (slow addition of *i*-PrOH until the solution became turbid followed by centrifugation, 4,000 rpm for 15 min.). Five fractions were isolated and dried in vacuo at room temperature.

The core diameter of CdTe@TGA QDs fraction used in this work was ca. 2.5 nm (estimated by transmission electron and atomic force microscopies) with a fluorescence emission peak at 602 nm.

Surface functionalization of CdTe@TGA QDs with saccharides

Galactose (Gal), mannose (Man) or glucose (Glu) (Fig. 1) were adsorbed at the surface of QDs by incubation of a 0.01 M solution of the desired saccharide with a 500 nM aqueous solution of CdTe@TGA QDs at room temperature for 15 min. Two saccharide/QDs molar ratio (1/5 and 1/1) were used in our experiments.

Yeast strains

Kluyveromyces bulgaricus and *Saccharomyces cerevisiae* were grown in Sabouraud liquid culture medium containing 1% Primatone (Sigma) and 2% glucose. The cultures were achieved aerobically at 25 °C in 100 mL flasks.

Materials characterization

All the optical measurements were performed at room temperature (20±2 °C) under ambient conditions. Absorption spectra were recorded on a Perkin-Elmer Lambda 2 UV-visible spectrophotometer. Fluorescence spectra were recorded on a F222 Jobin Yvon Fluorolog-3 spectrofluorimeter equipped with a thermostated cell compartment

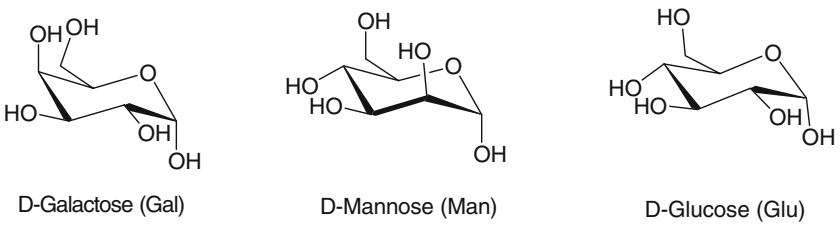

Fig. 1 Molecular structure of the saccharides employed

(25 °C), using a 450 W Xenon source. The quantum yields (QYs) were determined by the equation:

$$QY(sample) = \left(F_{sample}/F_{ref}\right)\left(A_{ref}/A_{sample}\right)\left(n_{sample}{}^2/n_{ref}{}^2\right)QY_{(ref)}$$

where F, A and n are the measured fluorescence (area under the emission peak), the absorbance at the excitation wavelength and the refractive index of the solvent, respectively. Photoluminescence (PL) spectra were spectrally corrected and quantum yields were determined relative to Rhodamine 6G in ethanol (QY=94%) [38].

To determine the morphology and the diameters of the nanoparticles, the samples were analyzed ex situ by Atomic Force Microscopy (AFM) and by Transmission Electron Microscopy (TEM). AFM characterization was carried out using a Digital Instruments Nanoscope III. AFM measurements of the surface topology were carried out in taping mode using a Si_3N_4 tip with resonance frequency and spring constant being 100 kHz and 0.6 $N.m^{-1}$. TEM images were taken by placing a drop of the particles in water onto a carbon film supported copper grid. Samples were studied using a Philips CM20 instrument with LaB_6 cathode operating at 200 kV. X-ray powder diffraction (XRD) spectra were taken on a Rotaflex RU-200B, RIGAKU generator and CPS 120 INEL detector, transmission assembly, Cu Kα radiation (λ=1.5418 Å).

Dynamic light scattering (DLS) was performed at room temperature using a Malvern zetasizer HsA instrument with an He-Ne laser (4 10^{-3} W) at a wavelength of 633 nm. The QDs aqueous solutions were filtered through Millipore membranes (0.2 μm pore size). The data were analyzed by the CONTIN method to obtain the hydrodynamic diameter (d_H) and the size distribution in each aqueous dispersion of nanoparticles.

Fluorescent microscopic observations were performed using a Zeiss Axioscope 50 microscope equipped with a Zeiss MC 80 camera. An excitation filter at 360 nm and an emission filter at 576 nm were used to observe probes bound on the cells.

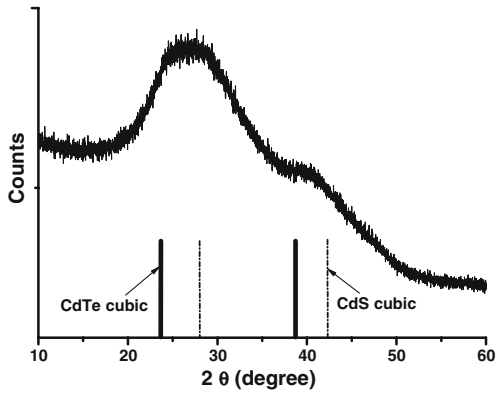

Fig. 2 XRD pattern of CdTe@TGA QDs synthesized at 100 °C. The standard diffraction lines of cubic CdTe and cubic CdS are also shown at the bottom

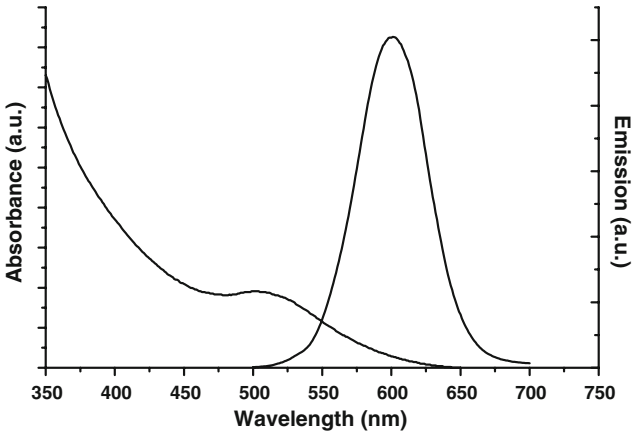

Fig. 3 Absorption and emission spectra of the CdTe@TGA QDs fraction isolated after size-selective precipitation with *i*-PrOH

Results and discussion

Characterization of unfunctionalized and of saccharides-functionalized CdTe@TGA QDs

A typical XRD pattern of the TGA-coated CdTe nanocrystals is shown on Fig. 2. The lattice parameters derived from XRD results demonstrate that the nanocrystals belong to the cubic zinc blende structure. The XRD peak positions are located between those of a pure cubic CdTe crystal and a pure CdS crystal. This result indicates a decomposition of the TGA surface ligand in the course of the growth of the QDs at 100 °C and the incorporation of the sulfur released into the nanocrystals leading to core/shell CdTe/CdS QDs [39, 40].

Figure 3 shows the absorption and fluorescence spectra of CdTe@TGA QDs prepared by the aqueous synthetic approach. The starting particle sample used the current investigations exhibits a symmetrical emission centered at 602 nm, which gives rise to an orange fluorescence color upon excitation at 400 nm. Its photoluminescence quantum yield (PL QY) was 31% using Rhodamine 6G as fluorescence standard. The average diameter of nanoparticles determined by Transmission Electron Microscopy (TEM) and Atomic Force Microscopy (AFM) (Fig. 4) are 2.9±0.7 nm and 2.5±0.5 nm, respectively. These values are in good accordance with the value calculated using the published curve and the size-dependent molar extinction coefficient at the first absorption peak (λ_{abs}=504 nm, ε= 67,157 $cm^{-1}.mol^{-1}$, 2.45 nm) [41]. The diameter determined using TEM is slightly enhanced compared to that

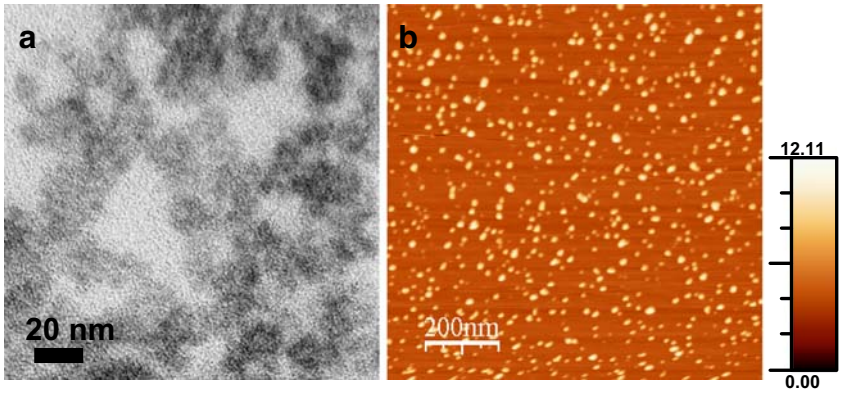

Fig. 4 TEM **a** and AFM **b** images of CdTe@TGA QDs after size-selective precipitation. The average diameters calculated (ca. 100 particles counted) are 3.4±0.7 and 2.8±0.5 nm, respectively

determined using AFM heights as AFM sizing of nanoparticles in air is very sensitive to attractive forces between the tip and the sample [42, 43]. The QDs were also investigated by dynamic light scattering (DLS). Figure 5 shows the number size distribution of starting CdTe@TGA QDs. The hydrodynamic diameter d_H of these nanoparticles is 8.5 nm with a narrow size distribution. The average diameter obtained via DLS is larger than the inorganic CdTe core as expected because DLS gives the diameter of the core, of the surface TGA ligands and of the associated hydration shell. The size distributions of Man-and Gal-functionalized CdTe@TGA QDs are similar to that of original QDs (data not shown), which confirms that surface functionalization has no influence on the physical state of the QDs.

It is generally considered that quantum yields are related to traps on the surface of CdTe QDs that mainly originate from Te atoms with dangling bonds [44]. The traps could be occupied by saccharides that can adhere to the surface of the QDs by electrostatic forces during the 15 min incubation. For this reason, a covalent anchorage of saccharides mediated by 1-ethyl-3-(3-dimethylaminopropyl)carbodiimide hydrochloride (EDC) and *N*-hydroxysuccinimide (NHS) was not followed. After the non-covalent conjugation of Glu, Man and Gal, the absorption maximum position at the first exciton peak (λ_{abs}=504 nm) remained constant. No fluorescence shift (λ_{em}=602 nm) was observed (Fig. 6). A weak increase of PL QYs (38, 37 and 34% for CdTe@TGA QDs modified with Glu, Man and Gal, respectively) was noticed compared to starting nanoparticles (PL QY=31%), thus confirming the bonding of saccharides onto the nanocrystals surface and the passivation of traps.

Epifluorescence microscopy experiments

Since nonspecific interactions of QDs with microorganisms have already been observed [45], the behavior of CdTe@TGA QDs towards yeast cells was examined first before further experiments. In a typical test, CdTe@TGA QDs were incubated with *K. bulgaricus* and *S. cerevisiae* cells for 15 min at room temperature. It was found out that both yeasts were only weakly stained by CdTe QDs (data not shown), indicating that CdTe@TGA QDs without surface bioconjugation have difficulty adhering to cells through nonspecific interactions.

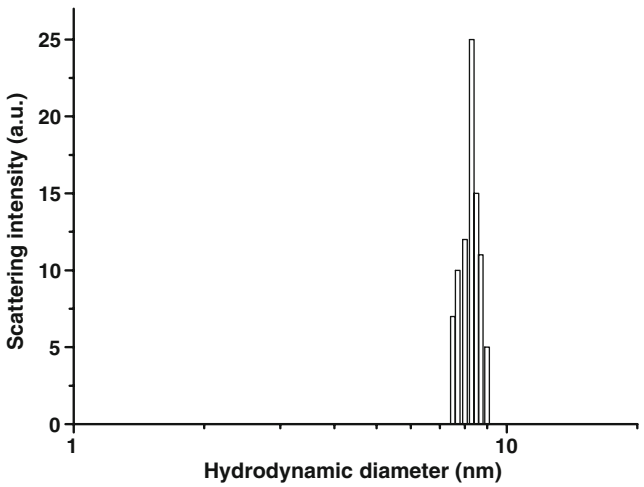

Fig. 5 Intensity-hydrodynamic size distribution graph of CdTe@TGA QDs in water at 25 °C

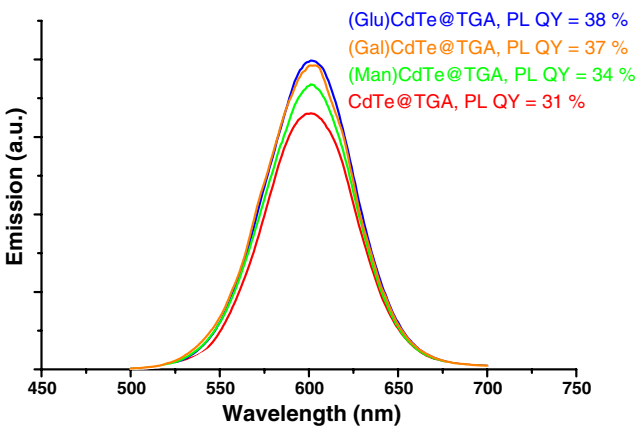

Fig. 6 PL spectra of CdTe@TGA QDs before and after absorption of Glu, Gal and Man (a saccharide/QDs molar ratio of 1/5 was used in the experiment)

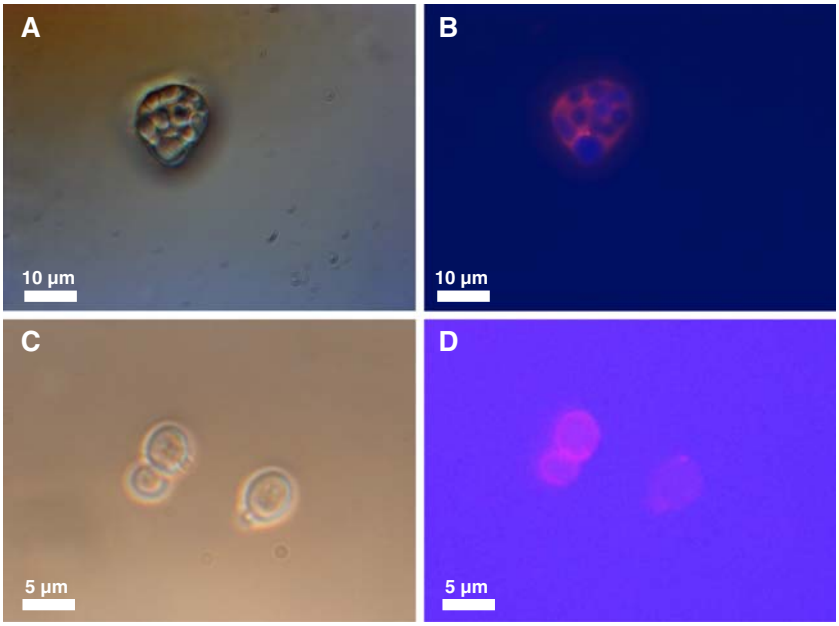

Fig. 7 Living yeasts labelled with sugar-functionalized CdTe@TGA nanocrystals. *S. cerevisiae* interaction with (Man)CdTe@TGA QDs, **a** light field image, and **b** the corresponding photoluminescence image. *K. bulgaricus* interaction with (Gal) CdTe@TGA QDs, **c** light field image, and **d** the corresponding photoluminescence image. The saccharide/QDs molar ratio was 1/5 in all experiments

In further experiments, sugar-conjugated QDs were incubated 15 min with yeast cells before pelleting at 14,000 rpm in a microcentrifuge and washing in 1% saline to eliminate medium fluorescence and unbound QDs. It is worthy to note that incubation times higher than 15 min did not modify the yeast cells-QDs association process. The suspension obtained after centrifugation was then analyzed by fluorescence microscopy to identify the success or the failure of the labelling and to get a rough estimate of the cellular localization of the fluorescence. Cells were examined live under a coverslip. Figure 7 shows that CdTe@TGA QDs associated to Man and Gal (referred to as (Man)CdTe@TGA and (Gal)CdTe@TGA) adhere to *S. cerevisiae* and *K. bulgaricus*, respectively. No differences were observed in labelling experiments using saccharide/QDs molar ratios of 1 to 5 or 1 to 1. Both sugar-conjugated QDs were homogenously distributed around the cell wall of yeasts. Sugar/lectin specificity was preserved with both (Man)CdTe@TGA and (Gal)CdTe@TGA QDs. When *S. cerevisiae* and *K. bulgaricus* cells incubated respectively with (Gal) CdTe@TGA and (Man)CdTe@TGA QDs were pelleted, most QDs remained in the supernatant. Optical microscopy showed that cells exhibited only weak fluorescence all around their outer surfaces (data not shown). Similar results were obtained with (Glu)CdTe@TGA QDs which neither is recognized by lectins and that preferentially localizes in the bud scars of *S. cerevisiae* (Fig. 8).

Conclusions

We have designed and prepared sugar-modified CdTe QDs that allowed to selectively label *S. cerevisiae* and *K. bulgaricus* yeast cells. The ease and rapidity of processing and the fair photoluminescence of the CdTe-sugar conjugated QDs provide a practical and economical approach for single-target-imaging applications and promise to be a versatile tool for fluorescence probing in complex biological systems.

Achnowledgements The authors thank Dr. Raphaël Duval (SRSMC-Nancy University) for facilitating imaging experiments.

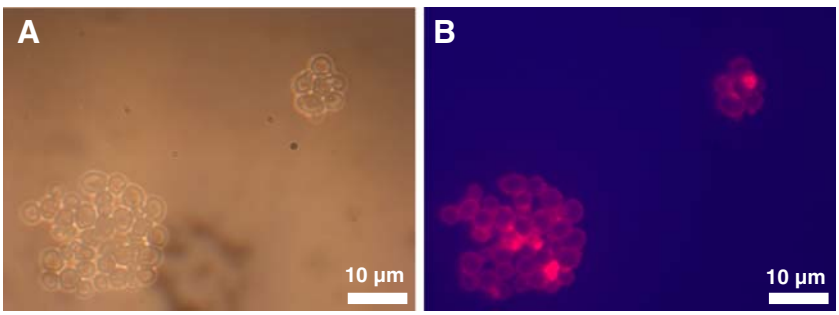

Fig. 8 *S. cerevisiae* interaction with (Glu)CdTe@TGA QDs, **a** light field image, and **b** the corresponding photoluminescence image

References

1. Bruchez MJr, Moronne M, Gin P, Weiss S, Alivisatos AP (1998) Semiconductor nanocrystals as fluorescent biological labels. Science 281:2013–2016
2. Chan WCW, Nie S (1998) Quantum dot bioconjugates for ultrasensitive nonisotopic detection. Science 281:2016–2018
3. Han M, Gao X, Su JZ, Nie S (2001) Quantum-dot-tagged microbeads for multiplexed optical coding of biomolecules. Nat Biotechnol 19:631–635
4. Medintz IL, Uyeda HT, Goldman ER, Mattoussi H (2005) Quantum dot bioconjugates for imaging, labelling and sensing. Nat Mater 4:435–446
5. Weng J, Ren J (2006) Luminescent quantum dots: a very attractive and promising tool in biomedicine. Curr Med Chem 13:897–909
6. Sun QJ, Wang YA, Li LS, Wang DY, Zhu T, Xu J, Yang CH, Li YF (2007) Bright, multicoloured light-emitting diodes based on quantum dots. Nat Photonics 1:717–722
7. Jamieson T, Bakhshi R, Petrova D, Pocock R, Imani M (2007) Biological applications of quantum dots. Biomaterials 28:4717–4732
8. Romero MJ, van de Lagemaat J, Mora-Sero I, Rumbles G, Al-Jassim MM (2006) Imaging of resonant quenching of surface plasmons by quantum dots. Nano Lett 6:2833–2837
9. Yong K-T, Roy I, Pudavar HE, Bergey EJ, Tramposch KM, Swihart MT, Prasad PN (2008) Multiplex imaging of pancreatic cancer cells by using functionalized quantum rods. Adv Mater 20:1412–1417
10. Michalet X, Pinaud FF, Bentolila LA, Tsay JM, Doose S, Li JJ, Sundaresan G, Wu AM, Gambhir SS, Weiss S (2005) Quantum dots for live cells, in vivo imaging, and diagnostics. Science 307:538–544
11. Hild WA, Breunig M, Goepferich A (2008) Quantum dots−Nano-sized probes for the exploration of cellular and intracellular targeting. Eur J Pharm Biopharm 68:153–168
12. Xu G, Yong K-T, Roy I, Mahajan SD, Ding H, Schwartz SA, Prasad PN (2008) Bioconjugated quantum rods as targeted probes for efficient transmigration across an in vitro blood−brain barrier. Bioconjugate Chem 19:1179–1185
13. Somers RC, Bawendi MG, Nocera DG (2007) CdSe nanocrystal based chem-/bio-sensors. Chem Soc Rev 36:579–591
14. Howarth M, Liu W, Puthenveetil S, Zheng Y, Marshall LF, Schmidt MM, Wittrup KD, Bawendi MG, Ting AY (2008) Monovalent, reduced-size quantum dots for imaging receptors on living cells. Nat Methods 5:397–399
15. Liu W, Howarth M, Greytak AB, Zheng Y, Nocera DG, Ting AY, Bawendi MG (2008) Compact biocompatible quantum dots functionalized for cellular imaging. J Am Chem Soc 130:1274–1284
16. PMA De farias, Santos BS, Menezes FD, Brasil AGJr, Ferreira R, Motta MA, Castro-Neto AG, Vieira AAS, Silva DCN, Fontes A, Cesar CL (2007) Highly fluorescent semiconductor core-shell CdTe-CdS nanocrystals for monitoring living yeast cells activity. Appl Phys A 89:957–961
17. Niikura K, Nishio T, Akita H, Matsuo Y, Kamitani R, Kogure K, Harashima H, Ijiro K (2007) Accumulation of *O*-GlcNAc-displaying CdTe quantum dots in cells in the presence of ATP. ChemBioChem 8:379–384
18. Higuchi Y, Oka M, Kawakami S, Hashida M (2008) Mannosylated semiconductor quantum dots for the labeling of macrophages. J Control Release 125:131–136
19. Jiang X, Ahmed M, Deng Z, Narain R (2009) Biotinylated glyco-functionalized quantum dots: synthesis, characterization, and cytotoxicity studies. Bioconjugate Chem 20:994–1001
20. Kikkeri R, Lepenies B, Adibekian A, Laurino P, Seeberger PH (2009) In vitro imaging and in vivo liver targeting with carbohydrate capped quantum dots. J Am Chem Soc 131:2110–2112
21. Mukhopadhyay B, Martins MB, Karamanska R, Russell DA, Field RA (2009) Bacterial detection using carbohydrate-functionalised CdS quantum dots: a model study exploiting E. coli recognition of mannosides. Tetrahedron Lett 50:886–889
22. Chen Y, Ji T, Rosenzweig Z (2003) Synthesis of glyconano-spheres containing luminescent CdSe—ZnS quantum dots. Nano Lett 3:581–584
23. Osaki F, Kanamori T, Sando S, Sera T, Aoyama Y (2004) A quantum dot conjugated sugar ball and its cellular uptake. On the size effects of endocytosis in the subviral region. J Am Chem Soc 126:6520–6521
24. Robinson A, Fang J-M, Chou P-T, Liao K-W, Chu R-M, Lee S-L (2005) Probing lectin and sperm with carbohydrate-modified quantum dots. ChemBioChem 6:1899–1905
25. Gill R, Bahshi L, Freeman R, Willner I (2008) Optical detection of glucose and acetylcholine esterase inhibitors by H_2O_2-sensitive CdSe/ZnS quantum dots. Angew Chem Int Ed 47:1676–1679
26. Babu P, Sinha S, Surolia A (2007) Sugar−quantum dot conjugates for a selective and sensitive detection of lectins. Bioconjugate Chem 18:146–151
27. Al-Mahmood S, Colin S, Bonaly R (1991) Kluyveromyces bulgaricus yeast lectins. Isolation of two galactose-specific lectin forms from the yeast cell wall. J Biol Chem 266:20882–20887
28. El-Behhari M, Géhin G, Coulon J, Bonaly R (2000) Evidence for a lectin in Kluyveromyces sp. that is involved in co-flocculation with Schizosaccharomyces pombe. FEMS Microbiol Lett 184:41–46
29. Géhin G, Coulon J, Coleman A, Bonaly R (2001) Isolation and biochemical characterization of cell wall tight protein complex involved in self-flocculation of Kluyveromyces bulgaricus. Antonie van Leeuwenhock 80:225–236
30. Miki BL, Poon SH, Seligy VL (1982) Possible mechanism for flocculation interactions governed by gene FLO1 in Saccharomyces cerevisiae. J Bacteriol 150:878–889
31. Kuriyama H, Umeda I, Kobayashi H (1991) Role of cations in the flocculation of Saccharomyces cerevisiae and discrimination of the corresponding proteins. Can J Microbiol 37:397–403
32. Javadekar VS, Sivaraman H, Sainkar SR, Khan MI (2000) A mannose-binding protein from the cell surface of flocculent Saccharomyces cerevisiae (NCIM 3528): its role in flocculation. Yeast 16:99–110
33. Straver MH, Traas VM, Smit G, Kijne JW (1994) Isolation and partial purification of mannose-specific agglutinin from brewer's yeast involved in flocculation. Yeast 10:1183–1193
34. Viard B, Al-Mahmood S, Streiblova E, Bonaly R (1993) Alternate interactions of the D-galactose-specific yeast lectin Kb-CWL I with sensitive yeast strains. FEMS Microbiol Lett 107:17–23
35. Coulon J, Thiebault F, Contino C, Polidora A, Bonaly R, Pucci B (2000) Permeability of yeast cell envelope to fluorescent galactosylated telomers derived from THAM Bioconjugate. Chem 11:461–468
36. Li L, Qian H, Fang N, Ren J (2006) Significant enhancement of the quantum yield of CdTe nanocrystals synthesized in aqueous phase by controlling the pH and concentrations of precursor solutions. J Luminescence 116:59–66
37. Aldeek F, Balan L, Lambert J, Schneider R (2008) The influence of capping thioalkyl acid on the growth and photoluminescence efficiency of CdTe and CdSe quantum dots. Nanotechnology 19:475401
38. Crosby GA, Demas JN (1971) Measurement of photoluminescence quantum yields. Review J Phys Chem 75:991–1024
39. Gao M, Kirstein S, Möhwald H, Rogach AL, Kornowski A, Eychmüller A, Weller H (1998) Strongly photoluminescent CdTe

nanocrystals by proper surface modification. J Phys Chem B 102:8360–8363
40. Li L, Qian HF, Ren JC (2005) Rapid synthesis of highly luminescent CdTe nanocrystals in the aqueous phase by microwave irradiation with controllable temperature. Chem Commun 4:528–530
41. Lu WW, Qu LH, Guo WZ, Peng XG (2003) Experimental determination of the extinction coefficient of CdTe, CdSe, and CdS nanocrystals. Chem Mater 15:2854–2860
42. Ebenstein Y, Nahum E, Banin U (2002) Tapping mode atomic force microscopy for nanoparticle sizing: Tip—sample interaction effects. Nano Lett 2:945–950
43. Pinaud F, King D, Moore H-P, Weiss S (2004) Bioactivation and cell targeting of semiconductor CdSe/ZnS nanocrystals with phytochelatin-related peptides. J Am Chem Soc 126:6115–6123
44. Borchert H, Talapin DV, Gaponik N, Mc Ginley C, Adam S, Lobo A, Möller T, Weller H (2003) Relations between the photoluminescence efficiency of CdTe nanocrystals and their surface properties revealed by synchrotron XPS. J Phys Chem B 107:9662–9668
45. Lei Y, Jiang C, Liu S, Miao Y, Zou B (2006) A clean route for preparation of CdTe nanocrystals and their conjugation with bacterium. J Nanosci Nanotech 6:3784–3788